JPP Journal of Pharmacy and Pharmacology

JPP 2006, 58: 403–407

Received May 5, 2005
Accepted November 21, 2005
DOI 10.1211/jpp.58.3.0016
ISSN 0022-3573

Metabolism of nicotine in rat lung microvascular endothelial cells

Yoshinori Ochiai, Eiichi Sakurai, Akio Nomura, Kunio Itoh and Yorihisa Tanaka

Abstract

The aim of this study was to examine whether cultured rat lung microvascular endothelial cells (LMECs), which constitute the gas–blood barrier, have the ability to metabolize nicotine. Nicotine was biotransformed to cotinine and nicotine *N*′-oxide by cytochrome 450 (CYP) and flavin-containing monooxyganase (FMO), respectively, in rat LMECs. The intrinsic clearance (V_{max1}/K_{m1}) for the cotinine formation was about 20 times as high as that for the *trans*-nicotine *N*′-oxide formation in the low-K_m phase, indicating that oxidation by CYP was much higher than that by FMO. On the other hand, as shown in Eadie–Hofstee plots, the formation of *cis*-nicotine *N*′-oxide was monophasic, whereas the plot for the *trans*-nicotine *N*′-oxide formation was clearly biphasic. These results suggest that nicotine *N*′-oxide was stereoselectively metabolized to *cis* and *trans* forms. However, in the high-K_m phase there was no significant difference in *N*′-oxidation between the *cis* and *trans* forms. Moreover, we suggest that CYP2C11 and CYP3A2 are key players in the metabolism to cotinine of nicotine in rat LMECs using the respective enzyme inhibitors (tranylcypromine and troleandomycine). On the other hand, methimazole (5 μM) caused 73 and 45% decreases in the formation of *N*′-oxides of *cis*- and *trans*- enantiomers, respectively, demonstrating the presence of FMO in rat LMECs. These results suggest that rat LMEC enzymes can convert substrates of exogenous origin such as nicotine for detoxication, indicating LMECs are an important barrier for metabolic products, besides hepatic cells.

Introduction

Although there are many alkaloids in tobacco which may be of pharmacologic importance, the major one is nicotine. This compound is converted to several oxidative metabolites in the liver. The primary metabolites of nicotine are cotinine and nicotine *N*′-oxide. Cotinine is catalysed by cytochrome P450s (CYPs) and nicotine *N*′-oxide is catalysed by flavin-containing monooxygenase (FMOs). FMOs are microsomal enzymes that catalyse the NADPH- and O_2-dependent oxidation of many nitrogen-, sulfur-, selenium- and phosphorus-containing compounds, suggesting the enzyme responsible for *cis* and *trans N*′-oxidation of nicotine.

Nicotine inhaled in tobacco smoke enters the blood almost as rapidly as after rapid intravenous injection except the entry point into the circulation is pulmonary rather than systemic venous. The lung is a heavily vascularized organ and the gas–blood barrier in the lung is made of single layers of epithelial and endothelial cells (Kayyali et al 2003); therefore nicotine crosses the epithelial–endothelial barrier in the lung. Endothelial cells also comprise nearly 50% of the total cellular population of the lungs (Crapo et al 1978), and the microvascular endothelial cells have unique and efficient protective systems controlling the passage of materials. The first one is a permeability barrier and the second seems to be a metabolic barrier, formed by the enzymes in the endoplasmic reticulum of endothelial cells which metabolize some of the permeable molecules recognized as substrates. In fact, although endothelial cells have previously been shown to be important regulators of amino acid (Mann et al 1989; Herskowitz et al 1991) and purine (Kayyali et al 2003) metabolism, little is known about drug metabolism in lung microvascular endothelial cells (LMECs) in particular. However, since nicotine is lipophilic, nicotine that appears in the plasma will be easily accumulated in lipid-rich tissues such as the brain. The presence of drug-metabolizing enzymes (CYPs and FMOs)

Department of Pharmaceutics I, Tohoku Pharmaceutical University, 4-4-1 Komatsushima, Sendai 981-8558, Japan

Yoshinori Ochiai, Kunio Itoh, Yorihisa Tanaka

Department of Pharmaceutics, Faculty of Pharmaceutical Sciences, Aomori University, 2-3-1 Kobata, Aomori 030-0943, Japan

Eiichi Sakurai, Akio Nomura

Correspondence: Eiichi Sakurai, Department of Pharmaceutics, Faculty of Pharmaceutical Sciences, Aomori University, 2-3-1 Kobata, Aomori 030-0943, Japan. E-mail: esakurai@aomori-u.ac.jp

in LMECs may therefore prevent the entry of nicotine to the circulating system, besides hepatic metabolism.

In the present study, we examined whether cultured rat LMECs have the ability to metabolize nicotine using enzyme inhibitors or inactivation techniques.

Materials and Methods

Materials

Cis- and *trans*-nicotine *N*′-oxides were synthesized as described by Craig & Purushothaman (1970), and separated by HPLC as described below. Nicotine, glucose 6-phosphate dehydrogenase, NADP, glucose 6-phosphate and sodium 1-heptanesulfonate were obtained from Wako Pure Chemicals (Osaka, Japan). Cotinine, troleandomycine, tranylcypromine, gentamicin sulfate and amphotericin B were purchased from Sigma-Aldrich (St Louis, MO, USA). Dulbecco's modified Eagle's medium: nutrient mixture F-12 (D-MEM/F-12), heparin, piperazine-N′-(2-ethane-sulfonic acid) (HEPES), dispase, epidermal growth factor (EGF), fetal bovine serum (FBS) and donor horse serum (HS) were obtained from Gibco BRL, Life Technologies (Rockville, MD). Percoll was purchased from Pharmacia (Uppsala, Sweden). Collagenase P was obtained from Boehringer Mannheim (Mannheim, Germany). All other chemicals were of reagent grade and were obtained commercially.

Isolation and culture of rat LMECs

Three-week-old male Wistar rats purchased from Japan SLC (Hamamatsu, Japan) were housed at constant temperature (23 ± 1°C) and constant humidity (55 ± 5%), with automatically controlled lighting (07:00–19:00). Rat LMECs were isolated using a technique described previously (Magee et al 1994; Sakurai et al 2002). Twenty rats were killed by decapitation. The lungs were removed and placed in a beaker containing M199 solution with 0.005% antibiotic solution. The visceral pleura were first stripped from each lobe and the outer 3–5 mm of the peripheral lung tissue was dissected free of the remaining tissue. The pooled pieces of lung periphery were finely minced, washed with M199 and the fragments were collected on 40-μm nylon mesh. With constant gentle mechanical agitation the tissue was digested with 0.6% collagenase in M199 at 37°C for 20 min, and then incubated with 2.1% dispase in M199 at 37°C for 30 min. The suspension was mixed in M199 with 5% FBS. After centrifugation at $600 \times g$ for 10 min, the resulting tissue pellet was resuspended in M199 and filtered through 100-μm mesh. The microvessels were collected by centrifugation at $600 \times g$ for 10 min and resuspended in M199. The suspension was layered on a Percoll gradient formed by centrifugation of 50% Percoll at $26000 \times g$ at 4°C for 60 min and then centrifuged at $600 \times g$ for 10 min. After Percoll gradient centrifugation three layers were observed. The endothelial cells aggregates formed a band around the middle third of the gradient, and the entire middle layer was collected from gradients. The cells were resuspended in M199 and collected by centrifugation at $600 \times g$ for 10 min. The cell suspensions were seeded onto collagen-coated 225 cm^2 tissue culture flasks (Iwaki Glass, Funabashi, Japan). Cells were allowed to attach and grow to monolayers at 37°C in a humidified atmosphere of 5% CO_2/95% air. The culture medium (D-MEM/F-12 containing 14 mM of sodium bicarbonate, 20 ng mL^{-1} of EGF, 50 μg mL^{-1} of gentamycin–amphotericin B solution, 10 U mL^{-1} of heparin, 5% FBS and 5% HS) was changed every 3 days. Subculture was performed when the cells reached confluence, after approximately 6–7 days. Cells were trypsinized at a ratio of 1:3 after reaching confluence using 0.025% trypsin in HBSS containing 0.02% EDTA. Secondary subcultured cells (5×10^5 cells cm^{-2}) were grown on collagen-coated 225 cm^2 tissue culture flasks. All metabolism experiments were performed on only second passaged LMECs after cells reached confluence, in approximately 4 to 5 days.

Enzyme assay

For the enzyme kinetic studies, the cultured rat LMECs were homogenized in 0.1 M phosphate buffer (pH 7.4). Incubation vessels contained rat LMECs (0.25 mg protein mL^{-1}), $MgCl_2$ (25 mM), glucose 6-phosphate (6.7 mM), nicotine amide (2.5 mM) and glucose 6-phosphate dehydrogenase (1 unit mL^{-1}) in a total volume of 2 mL. Nicotine-dissolved 0.1 M phosphate buffer (pH 7.4) was the substrate at a final concentration in the range 0.25 to 2 mM. After addition of NADP (0.5 mM in 0.1 M phosphate buffer), the mixtures were incubated for 2 min at 37°C in a shaking water bath. At the end of the incubation, 7.0 mL of 2:1, v/v, mixture of isopropanol–dichloromethane was added as a reaction stopper. The mixture was vigorously shaken for 10 min and centrifuged for 10 min at $800 \times g$. The organic layer (5 mL) was evaporated to dryness under N_2. The residues were redissolved in 200 μL of the mobile phase of HPLC as described below; 20 μL was injected on to an HPLC column. Cotinine and nicotine *N*′-oxides of both forms were determined by HPLC using a modification of the technique described by Nakajima et al (1998a) as shown below.

Inhibition study

In order to characterize cytochrome P450 isoforms in rat LMECs, tranylcypromine and troleandomycine were used, respectively, for inhibition of CYP2C11 and CYP3A2, which are, respectively, male-specific and male-predominant in rat liver. Methimazole was also used for the inhibition study of FMO. The metabolism of nicotine (1 mM) was examined with or without each cytochrome P450 inhibitor (20 μM) and FMO inhibitor (5 μM) by the method described above. The concentrations used of these inhibitors are specific for inhibition of CYPs (CYP2C11 and CYP 3A2) and FMO. Inhibitors were added as tetrahydrofuran solutions (final concentration of 1%) and an equal volume of tetrahydrofuran was added to the control group.

HPLC conditions

HPLC was performed with a Shimazdu (Kyoto, Japan) LC-6A apparatus equipped with a UV detector (Shimazdu SPD-6A, Kyoto, Japan) and a CapcellPAK C18 SG column (150×4.6 mm i.d., 5 μm particle size, Shiseido, Tokyo, Japan). Material was

eluted with 750:1, v/v, acetonitrile–acetic acid containing 10 mM sodium heptanesulfonate at a flow rate of 1 mL min^{-1} at 30°C, and the absorption at 254 nm was measured. The peak of authentic nicotine and its metabolites cotinine and nicotine *N*′-oxides of *cis* and *trans* forms were symmetrical and clearly separated from other peaks. The calibration curves for metabolites were linear over the concentration range 50 μg mL^{-1} and the lower limit for quantitation was 0.1 μg mL^{-1}.

Data analysis

The formation of metabolites from nicotine was calculated as nmol formed min^{-1} (mg protein)$^{-1}$. The kinetic data were fitted to the Michaelis–Menten equation for a one-enzyme or two-enzyme system using the non-linear least-squares regression analysis program MULTI, and apparent K_m and V_{max} values were estimated. Values are presented as mean ± s.e.m. of means for n experiments. Comparisons of data among groups were carried out using analysis of variance and Dunnett's post hoc multiple-comparisons test. Differences were considered significant at $P < 0.05$ (two-tailed).

Results

Figure 1 shows the relationship between the initial formation rates of cotinine and nicotine *N*′-oxide from nicotine incubated with rat LMECs and the concentration of nicotine (0.18–2.0 mM). The apparent K_m and V_{max} values for oxidation are listed in Table 1. Nicotine was biotransformed to cotinine in rat LMECs, and the Eadie–Hofstee plot for the cotinine formation was biphasic (Figure 1A), i.e. the summation of a low-K_m phase and a high-K_m phase (Table 1). Moreover, nicotine *N*′-oxide was stereoselectively formed. As shown in the Eadie–Hofstee plots, the formation of *cis*-nicotine *N*′-oxide was analysed to be monophasic, whereas the plot for the *trans*-nicotine *N*′-oxide formation was clearly biphasic (Figure 1B). On the other hand, the clearance value (V_{max1}/K_{m1}) for the cotinine formation was about 20 times as high as that for the nicotine *N*′-oxide formation in the low-K_m phase, indicating that oxidation by cytochrome P450 was much higher than that by FMO. However, in the high-K_m phase, the clearance value by *trans*-*N*′-oxidation was about same that by *cis*-*N*′-oxidation.

The effects of enzyme inhibitors on CYP and FMO activities were examined to determine the contribution of CYP and FMO enzymes in rat LMECs (Table 2 and 3). The addition of tranylcypromine (20 μM) and troleandomycine (20 μM) caused 56.5 and 36.4% inhibitions, respectively, of the formation of cotinine from nicotine. On the other hand, the formations of *cis*- and *trans*-nicotine *N*′-oxides were suppressed to 27 and 55% of the control value, respectively, by methimazole (5 μM).

Discussion

Nicotine is ingested by cigarette smoking and appears in the blood. However, because the accumulation in tissues of absorbed nicotine has toxic effects, the transfer to the blood of nicotine may be limited in the microvascular endothelial cells that constitute the gas–blood barrier in the lung. The importance of drug biotransformation in endothelial cells is now being recognized and several investigators report CYP-dependent drug oxidation activity in endothelial cells; induction of endothelial CYP monooxygenases can be achieved on treatment with various chemical agents (Farin et al 1994; Graier et al 1995; Stegemann et al 1995; Adeagbo 1997). It is therefore highly interesting to explore the contribution of rat LMECs in the lung-specific metabolism of nicotine. In this study, we have quantified the activities of two key nicotine metabolizing enzymes, CYP and FMO, and have also characterized CYP isoforms in cultured rat LMECs.

Our results indicate that cotinine is dominantly formed from nicotine, whereas nicotine *N*′-oxides are relatively minor metabolites in rat LMECs. Although human and rat

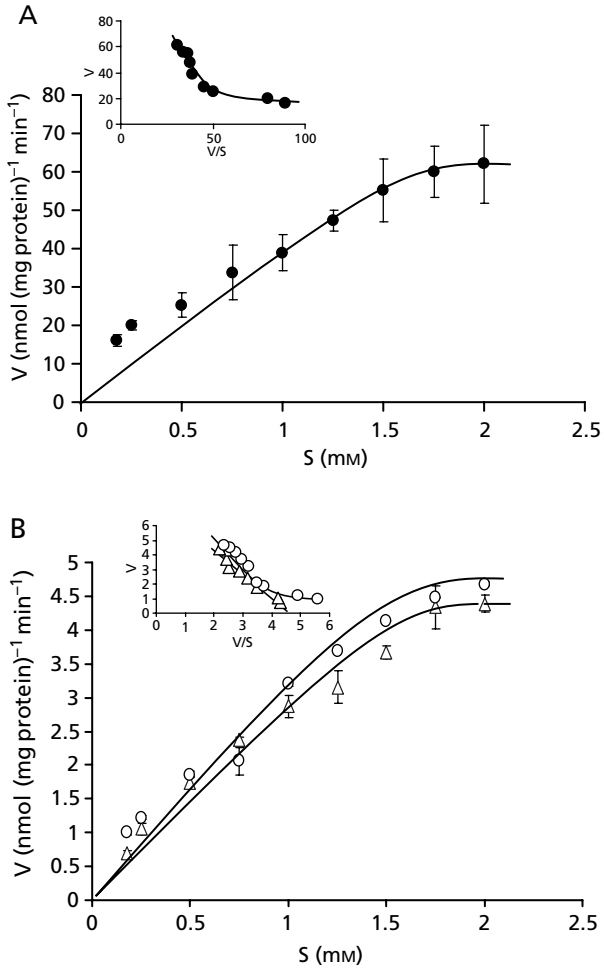

Figure 1 Michaelis–Menten plots for the formation of cotinine (A: ●) and nicotine *N*′-oxides (B: Δ, *cis* form; ○, *trans* form) from nicotine incubated with homogenized rat LMECs. Nicotine metabolism for 2 min at concentrations between 0.18 and 2.0 mM was determined at 37°C. Inset: the Eadie–Hofstee plots. Each point represents the mean ± s.e.m. of three experiments. V, metabolite formation rate (nmol (mg protein)$^{-1}$ min^{-1}); S, nicotine concentration (mM).

Table 1 Kinetic parameters for nicotine metabolism in rat LMECs

Low-K_m phase	**K_{m1} (mM)**	**V_{max1} (nmol (mg protein)$^{-1}$ min^{-1})**	**V_{max1}/K_{m1} (mL (mg protein)$^{-1}$ min^{-1})**
Cotinine	0.25 ± 0.02	39.1 ± 3.86	155.6 ± 11.2
cis-nicotine *N*′-oxide	–	–	–
trans-nicotine *N*′-oxide	0.57 ± 0.04	4.03 ± 0.23	7.1 ± 0.9
High-K_m phase	**K_{m2} (mM)**	**V_{max2} (nmol (mg protein)$^{-1}$ min^{-1})**	**V_{max2}/K_{m2} (mL (mg protein)$^{-1}$ min^{-1})**
Cotinine	1.61 ± 0.13	111.1 ± 9.24	69.0 ± 5.21
cis-nicotine *N*′-oxide	1.69 ± 0.01	7.87 ± 0.06	4.66 ± 0.11
trans-nicotine *N*′-oxide	1.74 ± 0.08	8.85 ± 0.92	5.09 ± 2.11

For nicotine metabolism in the rat, LMECs represent K_{m1} and V_{max1} apparent affinity constant and apparent maximum metabolic activity for the low-K_m phase, and K_{m2} and V_{max2} represent apparent affinity constant and apparent maximum metabolic activity for the high-K_m phase. Each value is the mean ± s.e.m. of three experiments.

Table 2 Effect of various inhibitors on the formation of cotinine by CYP in rat LMECs

Inhibitor	**Cotinine formation (nmol (mg protein)$^{-1}$ min^{-1})**
Control	29.0 ± 6.7
Tranylcypromine (20 μM)	13.1 ± 0.9*
Troleandomycine (20 μM)	18.4 ± 1.2*

The cotinine formation rates were determined with nitopine (1mM) at 37°C for 2 min. Each value is the mean ± s.e.m. of three experiments. *$P < 0.01$, compared with control.

Table 3 Effect of methimazole on the formation of nicotine *N*′-oxide by FMO in rat LMECs

Inhibitor	**Formation (nmol (mg protein)$^{-1}$ min^{-1})**	
	cis-nicotine-*N*′-oxide	*trans*-nicotine-*N*′-oxide
Control	2.8 ± 0.2	3.2 ± 0.1
Methimazole (5 μM)	0.76 ± 0.05*	1.8 ± 0.2*

The nicotine *N*′-oxide formation rates were determined with nicotine (1 mM) at 37°C for 2 min. Each value is the mean ± s.e.m. of three experiments. *$P < 0.01$, compared with control.

liver microsomes are extensive in the formation to cotinine of nicotine, and also to a small extent in nicotine *N*′-oxide formation (Park et al 1993; Rodrigues et al 1994; Nakajima et al 1998a), the metabolic profile obtained by rat LMECs is similar to that obtained by rat liver.

As shown in Figure 1, the formation of cotinine in rat LMECs was analysed to be biphasic, i.e. the summation of a low-K_m phase and a high-K_m phase by a Eadie–Hofstee plot, suggesting at least two different types of CYPs. Thum et al (2000) also showed that rat aortic endothelial cells express several genes (CYP1A1, CYP2B1/2, CYP2C11 and CYP2E1) that code for drug-metabolizing enzymes. Recently, they also found CYP1A1, CYP2A6/7, CYP2A13, CYP2B6/7, CYP2C8, CYP2E1, CYP2J2 and cyclophilin (housekeeping gene) to be expressed in cultures of human coronary arterial endothelial cells, but transcript levels of other CYPs were below the limit of detection (Borlak et al 2003). In this report, characterization of the CYP isoenzymes involved in oxidation of nicotine was investigated using two inhibitors (tranylcypromine for CYP2C11 inhibition and troleandomycine for CYP 3A2, respectively). As shown in Table 2, we suggest that CYP2C11 and CYP3A2 are key players in the metabolism to cotinine of nicotine in rat LMECs. This result seems to be reflected in the Eadie–Hofstee plot. To confirm the presence of CYP2C11 and CYP3A2 in rat LMECs, further data on the expression of these CYPs will be necessary. In the rats, on the other hand, nicotine, administered in a nutritionally balanced liquid diet, at a level of 20 (low), 60 (medium) or 200 (high) mg kg^{-1} of the diet, induced CYP1A1 in the lung and kidney in a dose-dependent manner and in the liver at the high nicotine dose only (Iba et al 1999). Subchronically administered nicotine, at behaviourally relevant doses, also induces rat hepatic ethanol-metabolizing CYP2E1 (Schoedel & Tyndale 2003). Recently, it has also been reported that in the rat nicotine is metabolized to cotinine primarily by hepatic CYP2B1 (Miksys et al 2000). This enzyme is also found in other organs such as the lung and brain. Further studies should therefore investigate the involvement of CYP1A1, CYP2B1/2 and CYP2E1 by rat LMECs using various inducers.

On the other hand, as shown in Eadie–Hofstee plots, the formation of *cis*-nicotine *N*′-oxide is monophasic, whereas the plot for the *trans*-nicotine *N*′-oxide formation is clearly biphasic, suggesting stereoselective nicotine *N*′-oxidation by rat LMECs. In kinetic studies of nicotine *N*′-oxidation in rat liver microsomes, the formation of *cis*-nicotine *N*′-oxide was greater than that of *trans*-nicotine *N*′-oxide (Nakajima et al 1998b). However, in rat LMECs, there was no significant difference in nicotine *N*′-oxidation between *cis* and *trans* enantiomers in comparison to V_{max}/K_m in a high-K_m phase.

Methimazole also caused 73 and 45% decreases in the formation of *N*′-oxides of the *cis* and *trans* enantiomers, respectively, demonstrating the presence of FMO in rat LMECs. Five isoforms of FMO have been identified thus far (FMO1–FMO5) (Burnett et al 1994; Hines et al 1994). It is

also reported that FMO1 has been shown to be the major enzyme responsible for the formation of both *cis*- and *trans*-nicotine *N*′-oxides in the liver. FMO3 also catalyses the oxidation of several important drugs and xenobiotics such as methimazole, chlorpromazine and nicotine in human liver (Cashman et al 1995; Overby et al 1997). Moreover, only *trans*-nicotine *N*′-oxide can be solely oxidized by FMO2 and FMO3 (Park et al 1993), but a lack of functional FMO2 is demonstrated in rat lung by Lattard et al (2002). In our study, as shown in the Eadie–Hofstee plots, several types of FMOs may be involved in *N*′-oxidation of nicotine in rat LMECs. Further experimentation to characterize FMO isoenzymes in rat LMECs will therefore be necessary.

Conclusion

Rat LMEC enzymes can convert substrates of exogenous origin such as nicotine for detoxication, indicating LMECs are an important barrier for metabolic products besides a permeability barrier to the passage of materials (Sakurai et al 2002).

References

Adeagbo, A. S. (1997) Endothelium-derived hyperpolarizing factor: characterization as a cytochrome P450 1A-linked metabolite of arachidonic acid in perfused rat mesenteric prearteriolar bed. *Am. J. Hypertens*. **10**: 763–771

Borlak, J., Walles, M., Levsen, K., Thum, T. (2003) Verapamil: metabolism in cultures of primary human coronary arterial endothelial cells. *Drug Metab. Dispos*. **22**: 788–798

Burnett, V. L., Lawton, M. P., Philpot, R. M. (1994) Cloning and sequencing of flavin-containing monooxygenases FMO3 and FMO4 from rabbit and characterization of FMO3. *J. Biol. Chem*. **269**: 14314–14322

Cashaman, J. R., Park, S. B., Berkman, C. E., Cashman, L. E. (1995) Role of hepatic flavin-containing monooxygenase 3 in drug and chemical metabolism in adult humans. *Chem.-Biol. Interact*. **96**: 33–46

Craig, J. C., Purushothaman, K. K. (1970) An improved preparation of tertiary amine *N*-oxides. *J. Org. Chem*. **35**: 1721–1722

Crapo, J. D., Peters-Golden, M., March-Salin, J., Shelburne, J. S. (1978) Pathologic changes in the lungs of oxygen-adapted rats. *Lab. Invest*. **39**: 640–653

Farin, F. M., Pohlman, T. H., Omiecinski, C. J. (1994) Expression of cytochromes P450s and microsomal epoxide hydrolase in primary cultures of human umbilical vein endothelial cells. *Toxicol. Appl. Pharmacol*. **124**: 1–9

Graier, W. F., Simecek, S., Sturek, M. (1995) Cytochrome P450 mono-oxygenase-regulated signaling of Ca^{2+} entry in human and bovine endothelial cells. *J. Physiol*. **482**: 259–274

Herskowitz, K., Bode, B. P., Block, E. R., Souba, W. W. (1991) The effects of endotoxin on glutamine transport by pulmonary artery endothelial cells. *J. Surg. Res*. **50**: 356–361

Hines, R. N., Cashman, J. R., Philpot, R. M., Williams, D. E., Ziegler, D. M. (1994) The mammalian flavin-containing monooxygenases: molecular characterization and regulation of expression. *Toxicol. Appl. Pharmacol*. **125**: 1–6

Iba, M. M., Fung, J., Pak, Y. W., Thomas, P. E., Fisher, H., Sekowski, A., Halladay, A. K., Wagner, G. C. (1999) Dose-dependent upregulation of rat pulmonary, renal, and hepatic cytochrome P-450 (CYP) 1A expression by nicotine feeding. *Drug Metab. Dispos*. **27**: 977–982

Kayyali, U. S., Budhiraja, R., Pennella, C. M., Cooray, S., Lanzillo, J. J., Chalkley, R., Hassoun, P. M. (2003) Upregulation of xanthine oxidase by tobacco smoke condensate in pulmonary endothelial cells. *Toxicol. Appl. Pharmacol*. **188**: 59–68

Lattard, V., Longin-Sauvageon, C., Krueger, S. K., Williams, D. E. (2002) The FMO2 gene of laboratory rats, as in most humans, encodes a truncated protein. *Biochem. Biophys. Res. Commun*. **292**: 558–563

Magee, J., Stone, A. E., Oldham, K. T., Guice, K. S. (1994) Isolation, culture, and characterization of rat lung microvascular endothelial cells. *Am. J. Physiol. Lung Cell Mol. Physiol*. **267**: L433–L441

Mann, G. E., Pearson, J. D., Sheriff, C. J., Toothil, V. J. (1989) Expression of amino acid transport system in cultured human umbilical vein endothelial cells. *J. Physiol. Lond*. **410**: 325–339

Miksys, S., Hoffmann, E., Tyndale, R. F. (2000) Regional and cellular induction of nicotine-metabolizing CYP2B1 in rat brain by chronic nicotine treatment. *Biochem. Pharmacol*. **59**: 1501–1511

Nakajima, M., Iwata, K., Yamamoto, T., Funae, Y., Yoshida, T., Kuroiwa, Y. (1998a) Nicotine metabolism in liver microsomes from rats with acute hepatitis or cirrhosis. *Drug Metab. Dispos*. **26**: 36–41

Nakajima, M., Iwata, K., Yoshida, T., Yamamoto, T., Kuroiwa, Y. (1998b) Diastereospecific kinetics of nicotine N′-oxidation in rat liver microsomes. *Xenobiotica* **28**: 127–135

Overby, L. H., Carver, G. C., Philpot, R. M. (1997) Quantitation and kinetic properties of hepatic microsomal and recombinant flavin-containing monooxygenases 3 and 5 from human. *Chem.-Biol. Interact*. **106**: 29–45

Park, S. B., Jacob, P. 3rd, Benowitz, N. L., Cashman, J. R. (1993) Stereoselective metabolism of (S)-(–)-nicotine in humans: formation of trans-(S)-(–)-nicotine N-1′-oxide. *Chem. Res. Toxicol*. **6**: 880–888

Rodrigues, A. D., Ferrero, J. L., Amann, M. T., Rotert, G. A., Cepa, S. P., Surber, B. M., Machinist, J. M., Tich, N. R., Sullivan, J. P., Garvey, D. S. (1994) The in vitro hepatic metabolism of ABT-418, a cholinergic channel activator, in rats, dogs, cynomolgus monkey, and humans. *Drug Metab. Dispos*. **22**: 788–798

Sakurai, E., Sakurada, T., Ochiai, Y., Yamakami, J., Tanaka, Y. (2002) Stereoselective transport of histidine in rat lung microvascular endothelial cells. *Am. J. Physiol. Lung Cell Mol. Physiol*. **282**: L1192–L1197

Schoedel, K. A., Tyndale, R. F. (2003) Induction of nicotine-metabolizing CYP2B1 by ethanol and ethanol-metabolizing CYP2E1 by nicotine: summary and implications. *Biochim. Biophys. Acta* **1619**: 283–290

Stegemann, J. J., Hahn, M. E., Weisbrod, R., Woodin, B. R., Joy, J. S., Najibi, S., Cohen R. A. (1995) Induction of cytochrome P4501A1 by aryl hydrocarbon receptor agonists in porcine aorta endothelial cells in culture and cytochrome P4501A1 activity in intact cells. *Mol. Pharmacol*. **47**: 296–306

Thum, T., Haverich, A., Borlak, J. (2000) Cellular dedifferentiation of endothelium is linked to activation and silencing of certain nuclear transcription factors: implications for endothelial dysfunction and vascular biology. *FASEB J*. **14**: 740–751